

Our results support the view (2) that the ventricle transports chemicals applied to brain tissue. Such transport may bring the chemical to distant sites which, in turn, may mediate certain observed behavioral effects. The recent report of Baxter (11) is consistent with this view.

Because of the inability to fluoresce carbachol, we have not been able to assess its pattern of diffusion directly. Although it does not seem unreasonable to presume that carbachol, like dopamine, also enters the ventricle (2), autoradiographic studies may assist in evaluating this possibility. The inability to find any significant alteration of the normal fluorescent pattern after application of norepinephrine is somewhat puzzling but perhaps comprehensible in terms of mechanisms of rapid uptake recently described on the basis of autoradiographic techniques (12).

Our results demonstrate that chemicals are transported distances considerably greater than have heretofore assumed. Such results are clearly relevant to discussions of widespread behavioral effects of neurochemicals applied to brain (1). A combination of the techniques of fluorescence and chemical stimulation of brain may be valuable in studying the way in which neurochemicals are transmitted. Additionally, such information may shed light on the interactions among different neurochemicals. For example, if carbachol does become associated with the axon, it may subsequently cause the release of the transmitter located in the end button of the axon (13). This view might explain the occurrence of 2- to 5-minute latencies of behavioral effects which are sometimes observed after chemical stimulation of the brain.

ARYEH ROUTTENBERG

JOHN SLADEK

WILLIAM BONDAREFF

Departments of Psychology and
Anatomy, Northwestern University,
Evanston, Illinois 60201

References and Notes

1. S. P. Grossman, *Science* **132**, 301 (1960); A. E. Fisher and J. N. Coury, *ibid.* **138**, 691 (1962); R. A. Levitt and A. E. Fisher, *ibid.* **154**, 520 (1966); J. N. Coury, *ibid.* **156**, 1763 (1967); D. A. Booth, *ibid.* **158**, 515 (1967).
2. A. Routtenberg, *ibid.* **157**, 838 (1967).
3. R. D. Myers, *Physiol. Behav.* **1**, 171 (1966).
4. B. Falck and Ch. Owman, *Acta Univ. Lund II* **7**, 1 (1965).
5. J. H. Burn and M. J. Rand, *Nature* **184**, 163 (1959).
6. A. Routtenberg, *J. Exp. Anal. Behav.* **11**, 52 (1968).
7. ———, *Psychon. Sci.* **3**, 41 (1965).
8. H. Corrodi and G. Jonsson, *J. Histochem. Cytochem.* **15**, 65 (1967).
9. C. A. Taylor and P. Weiss, *Proc. Nat. Acad. Sci. U.S.A.* **54**, 1521 (1965); I. M. Korr, P. N.

- Wilkinson, F. W. Chornock, *Science* **155**, 342 (1967).
10. P. R. Lewis and C. C. D. Shute, *J. Cell Sci.* **1**, 381 (1966).
 11. B. L. Baxter, *Exp. Neurol.* **19**, 412 (1967).
 12. M. Reivich and J. Glowinski, *Brain* **90**, 633 (1967).

13. G. B. Koelle, in *The Pharmacological Basis of Therapeutics*, L. S. Goodman and A. Gilman, Eds. (Macmillan, New York, 1965).
14. Supported by PHS grant NB 07044, career award 1 K NB 4929 (W.B.), and grant MH 11991 (A.R.).

8 May 1968

Conformation and Activity of Chymotrypsin: The pH-Dependent, Substrate-Induced Proton Uptake

Abstract. Hydrogen ion uptake by chymotrypsin during reversible binding of specific substrate is shown to be due to an ionizing group of the enzyme with a $pK(\text{apparent}) \sim 9$ in the free enzyme. This $pK(\text{apparent})$ is shifted to a higher value in the enzyme-substrate complexes. Previous results indicating an equilibrium, controlled by this ionizing group, between active and inactive conformational forms of chymotrypsin are confirmed.

The experiments reported are part of an investigation of the mode of enzymic action of chymotrypsin (CT), which belongs to a group of hydrolytic enzymes including thrombin and acetylcholine esterase (1). The amino acid sequence of CT is known from the work of Hartley and of Keil and Sörm (2), and the conformation of crystalline α -CT has recently been deduced from x-ray diffraction studies by Blow and collaborators (3).

We have previously presented data which indicate that the reaction of CT with inhibitor (diisopropyl fluorophosphate) at alkaline pH is accompanied by an uptake of hydrogen ion by the enzyme (4), and this phenomenon has been confirmed by inhibition experiments in a number of laboratories (5-7). We have shown by both titration experiments (8) and kinetic studies (9) that an ionizing group of the enzyme

with $pK(\text{apparent}) \sim 9$ is implicated in this process. There is evidence (10) that this ionizing group is the amino-terminal isoleucyl α -amino group that is liberated in the conversion of chymotrypsinogen to active enzyme. We have, further, presented data which indicate the existence of pH-dependent equilibria between catalytically active and inactive conformations of the enzyme (9-13), the active conformation being stabilized by a positively charged α -amino group with $pK(\text{apparent}) \sim 9$. These equilibria between enzyme conformations are schematically presented in Fig. 1. The pH dependence of the enzyme-substrate dissociation constant (12, 14, 15) indicates that substrate binds better to the active conformation. Implications of these observations are that substrate binding must result in a stabilization of that enzyme conformation in which the crucial ionizing group

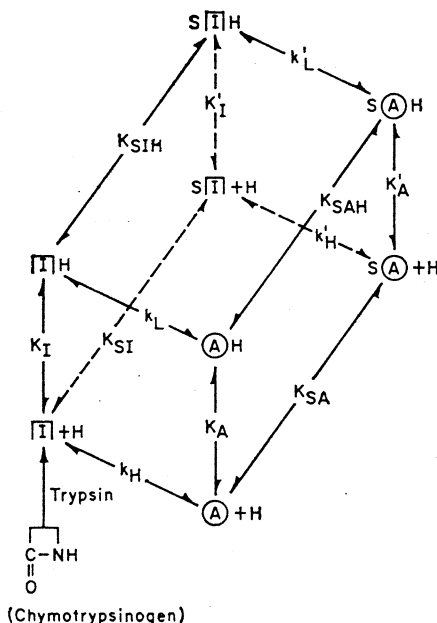


Fig. 1. Scheme showing equilibria between two main conformations of the enzyme, A (active) and I (inactive), in the free state and in complexes with substrate. S, and in protonated and unprotonated states of a critical ionizing group. A, AH, I, IH, SA, SAH, SI, and SIH represent the various protonated and unprotonated forms of enzyme and enzyme-substrate complexes. K_A and K_I are the acid dissociation constants of this ionizing group in the A and I conformations, respectively. This ionizing group controls the equilibria between enzyme conformations, equilibria characterized by the constants k_L , k_H , k'_L , and k'_H , where the subscript L refers to the conformation of the enzyme when the critical ionizing group is protonated (at pH 7), the subscript H refers to the high-pH form of the enzyme, and the prime refers to enzyme-substrate complex rather than free enzyme. K_{SA} , K_{SI} , K_{SAH} , and K_{SIH} are the various enzyme-substrate dissociation constants.

is protonated, and that the resulting shift between enzyme conformations must be accompanied by a hydrogen ion uptake by the enzyme. These predictions have now been confirmed in investigations, reported here, of the hydrogen ion uptake by CT which accompanies the reversible binding of a specific substrate, *N*-acetyl-L-tryptophanamide (L-ATA) and a specific inhibitor, *N*-acetyl-D-tryptophanamide (D-ATA).

The data are interpreted in terms of the scheme shown in Fig. 1. Equations relating the concentrations of the conformational forms of free enzyme and enzyme-substrate complexes to initial concentrations of enzyme and substrate and to the equilibrium constants have been given previously (10, 12). Complex ionization constants pertaining to both active and inactive conformational forms of free enzyme, E, and of the enzyme-substrate complexes, ES, may be expressed as:

$$K^*_{\text{E}} = \frac{(\text{I} + \text{A})(\text{H})}{(\text{IH} + \text{AH})} \cong K_{\text{A}} k_{\text{H}} \quad (1)$$

$$K^*_{\text{ES}} = \frac{(\text{SI} + \text{SA})(\text{H})}{(\text{SIH} + \text{SAH})} \cong K'_{\text{A}} k'_{\text{H}} \quad (2)$$

with symbols defined as in Fig. 1. The observed proton uptake per mole of enzyme that occurs upon binding of substrate is given by:

$$\Delta[\text{H}^+]_{\text{obs}} = \frac{[(\text{SAH} + \text{SIH} + \text{AH} + \text{IH})_{\text{S}_0 \text{ present}} - (\text{AH} + \text{IH})_{\text{S}_0 \text{ absent}}] [\text{E}_0]^{-1}}{\quad} \quad (3)$$

The quantities SAH, SIH, and so forth, can be expressed in terms of E_0 , S_0 , K^*_{E} , and K^*_{ES} , as previously shown (12). Substitution in Eq. 3 and rearrangement gives:

$$\Delta[\text{H}^+]_{\text{obs}} = \frac{\text{H}}{\text{H} + K^*_{\text{ES}}} \left[\left(1 + \frac{K_{\text{S}}}{\text{S}_0} \right) \times \left(1 + \frac{K_{\text{S}}(\text{H} + K^*_{\text{E}})}{\text{S}_0(\text{H} + K^*_{\text{ES}})} \right) - 1 \right] - \frac{\text{H}}{\text{H} + K^*_{\text{E}}} \quad (4)$$

where K_{S} is the apparent overall enzyme-substrate dissociation constant, H is hydrogen ion concentration, and other symbols are as defined in Fig. 1. With $K_{\text{m}}(\text{app})$ and $\Delta[\text{H}^+]_0$ defined as:

$$K_{\text{m}}(\text{app}) = K_{\text{S}} [(\text{H} + K^*_{\text{E}})/(\text{H} + K^*_{\text{ES}})] \quad (5)$$

$$\Delta[\text{H}^+]_0 = \frac{\text{H}}{\text{H} + K^*_{\text{ES}}} - \frac{\text{H}}{\text{H} + K^*_{\text{E}}} \quad (6)$$

Eq. 4 may be expressed as:

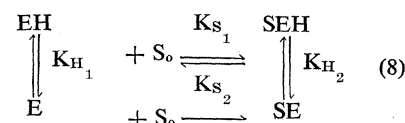
$$\Delta[\text{H}^+]_{\text{obs}} = \Delta[\text{H}^+]_0 - \frac{\Delta[\text{H}^+]_{\text{obs}} K_{\text{m}}(\text{app})}{\text{S}_0} \quad (7)$$

A representative plot, according to Eq. 4, of data obtained with δ -CT and L-ATA at pH 9.5, is shown in Fig. 2A. Such a plot yields $\Delta[\text{H}^+]_0$ as intercept and $K_{\text{m}}(\text{app})$ as slope. At corresponding pH levels, the $K_{\text{m}}(\text{app})$ values obtained from these studies are in excellent agreement with the $K_{\text{m}}(\text{app})$ values obtained from steady state measurements (12, 14), as required by the equations (12) pertaining to the Fig. 1 scheme. Plots of $\Delta[\text{H}^+]_0$ versus pH (Eq. 6) are shown in Fig. 2B. It should be noticed that $\Delta[\text{H}^+]_0$ goes through a maximum, $\Delta[\text{H}^+]_{\text{max}}$, at about pH 9.5.

The $K_{\text{m}}(\text{app})$ value for L-ATA and δ -CT increases by a factor of about 4 in the pH region 8 to 10 (12, 15). A fourfold increase in $K_{\text{m}}(\text{app})$ requires that K^*_{E} and K^*_{ES} differ correspondingly (see Eq. 5), and that $\Delta[\text{H}^+]_{\text{max}}$ be less than 1 (see Eq. 6), as is observed experimentally (Fig. 2B). The value of $K_{\text{m}}(\text{app})$ increases considerably more at alkaline pH for D-ATA and α -CT (16) than for L-ATA and δ -CT; this requires a correspondingly

larger separation in the values of K^*_{E} and K^*_{ES} (see Eq. 5), and hence greater proton uptake for α -CT than for δ -CT. The data in Fig. 2B indicate that these requirements are met. The data are satisfactorily explained by pK^*_{E} values of 9.0 for both enzyme forms in the absence of substrate, and pK^*_{ES} values of 9.6 for δ -CT and >10.0 for α -CT. An ionizing group with pK (apparent) ~ 9.0 has previously been implicated in the proton uptake by CT in its reaction with diisopropyl fluorophosphate (8, 9).

The simplest scheme which would account for these data is given by:



There is, however, a considerable amount of evidence (10, 11) that ionization of a single group of the enzyme is accompanied by conformational changes of CT, and that the scheme shown in Fig. 1 is appropriate. The

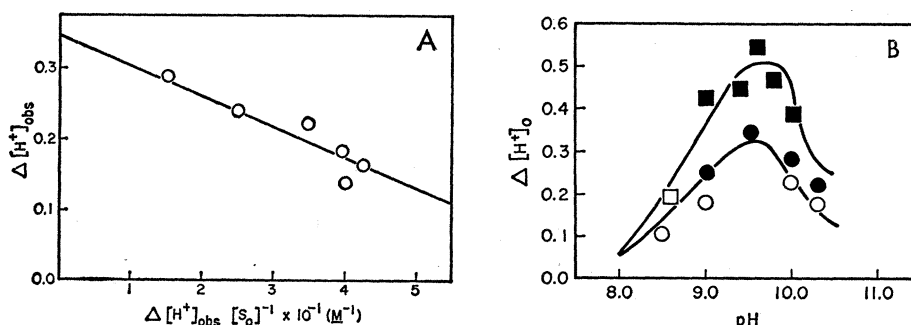


Fig. 2. The hydrogen ion uptake by enzyme which accompanies the binding of L-ATA to δ -CT and of D-ATA to α -CT. Equipment used includes a Radiometer pH meter (model TTT1c) with combination glass electrodes (A. H. Thomas, No. 4858-LI5), attached to a Tektronix storage oscilloscope (type 564) that is provided with an external potentiometer. The pH changes were recorded on the oscilloscope in terms of millivolts. Solutions of substrate, and subsequently of CT with the substrate added by means of a Hamilton gas-tight syringe (No. 1002), were measured in the same reaction vessel, which was stoppered, thermostatted, and flushed with nitrogen. The solutions of substrate and CT were approximately 2 ml in volume. The readings at each pH were converted to values of $\Delta[\text{H}^+]_{\text{obs}}$ with use of standard curves obtained by adding varying amounts of acid or base to enzyme solutions of appropriate concentrations and pH. Also, the $\Delta[\text{H}^+]_{\text{obs}}$ values were corrected on the basis of control experiments which were run for each experimental point in order to correct for any pH changes occurring in the solution as a result of the procedure. These control experiments consisted of carrying out the usual procedure with substitution of blank solutions of the same pH and salt concentration for the enzyme solution and for the substrate solution, and by running the experiment with chymotrypsinogen A in place of active enzyme. Concentrations of active enzyme were determined by active site titration with *N*-trans-cinnamoyl imidazole (17). All solutions were 0.1M in KCl. Temperature was $2.5^\circ \pm 0.1^\circ\text{C}$. (A) A plot of $\Delta[\text{H}^+]_{\text{obs}}/\text{S}_0$ according to Eq. 4. $\text{E}_0 = 7 \times 10^{-5}\text{M}$ δ -CT; $\text{S}_0 = 18.0$ to 2.3 mM L-ATA; pH = 9.5. Each experimental point represents at least three $\Delta[\text{H}^+]_{\text{obs}}$ determinations, obtained in different experiments with different enzyme preparations. The solid line has been computed by the method of least squares. (B) The pH dependence of $\Delta[\text{H}^+]_0$. Values of $\Delta[\text{H}^+]_0$ obtained in experiments such as the one illustrated in Fig. 2A, are plotted versus pH (filled symbols). Also shown are $\Delta[\text{H}^+]_{\text{obs}}$ values obtained at high substrate concentration ($\text{S}_0 = 18.3$ mM) (open symbols). The circles represent experiments with δ -CT and L-ATA, and the squares represent experiments with α -CT and D-ATA. The curves were calculated with use of a pK^*_{E} value of 9.0 for both enzymes, and pK^*_{ES} values of 9.6 and >10.0 for δ - and α -CT, respectively.

data presented here are consistent with the pH-dependent equilibrium between enzyme conformations shown in Fig. 1, and indicate that the complex ionization constants K^*_E and K^*_{ES} can be determined by application of the approach described in this paper.

JAMES MCCONN, EDMOND KU
CATHERINE ODELL
GEORGE CZERLINSKI
GEORGE P. HESS

Section of Biochemistry and
Molecular Biology, Cornell
University, Ithaca, New York 14850

References and Notes

1. D. E. Koshland, Jr., *Science* **142**, 1533 (1963).
2. B. S. Hartley, in *Structure and Activity of Enzymes*, T. W. Goodwin, J. I. Harris, B. S. Hartley, Eds. (Academic Press, New York, 1964), p. 47; B. Keil and F. Sörm, *ibid.*, pp. 24, 30.
3. B. W. Matthews, P. B. Sigler, R. Henderson, D. M. Blow, *Nature* **214**, 5089 (1967).

4. A. Y. Moon, J. M. Sturtevant, G. P. Hess, *Federation Proc.* **21**, 229 (1962).
 5. B. F. Erlanger, H. Castleman, A. G. Cooper, *J. Am. Chem. Soc.* **85**, 1872 (1963).
 6. J. Keizer and S. A. Bernhard, *Biochemistry* **5**, 4127 (1966).
 7. M. L. Bender and F. C. Wedler, Jr., *J. Am. Chem. Soc.* **89**, 3052 (1967).
 8. B. H. Havsteen and G. P. Hess, *Biochem. Biophys. Res. Comm.* **14**, 313 (1964).
 9. A. Y. Moon, J. M. Sturtevant, G. P. Hess, *J. Biol. Chem.* **240**, 4204 (1965).
 10. H. L. Oppenheimer, B. Labouesse, G. P. Hess, *ibid.* **241**, 2720 (1966).
 11. B. Labouesse, H. L. Oppenheimer, G. P. Hess, *Biochem. Biophys. Res. Comm.* **14**, 318 (1964).
 12. A. Himoe, P. C. Parks, G. P. Hess, *J. Biol. Chem.* **242**, 919 (1967).
 13. B. H. Havsteen and G. P. Hess, *J. Am. Chem. Soc.* **85**, 791 (1963).
 14. A. Himoe, P. C. Parks, G. P. Hess, *Federation Proc.* **24**, 473 (1965).
 15. A. Himoe and G. P. Hess, *Biochem. Biophys. Res. Comm.* **23**, 234 (1966).
 16. C. H. Johnson and J. R. Knowles, *Biochem. J.* **101**, 56 (1966).
 17. G. R. Schonbaum, B. Zerner, M. L. Bender, *J. Biol. Chem.* **236**, 2930, (1961).
 18. Supported by grants from NIH and NSF. J. McC. and E.K. are NIH postdoctoral fellows.
- 15 March 1968

Space-Filling Polyhedron: Its Relation to Aggregates of Soap Bubbles, Plant Cells, and Metal Crystallites

Abstract. A fourteen-faced space-filling polyhedron which closely approximates the actual distribution of four-, five- and six-sided polygons found in packings of soap bubbles and biological cells is proposed as an alternative to the Kelvin tetrakaidecahedron as the ideal polyhedron for these packings. This polyhedron may also have relevance to crystallite morphologies and crystal structures.

In nature, partitions of space into polyhedral cells by "close-packing" of bodies, such as aggregates of soap bubbles (1), plant cell tissue (2), and metal crystallites (3) tend to conform to at least three rules: (i) the average number of faces on aggregated bodies approaches 14 faces per body; (ii) the average number of sides per face is 5.143; and (iii) the vertices are generally tetrahedral, formed by four cells whose juncture angles are close to

$109^\circ 28'$ (4). The latter restriction is a consequence of the minimization of surface energy, which causes each body to enclose the greatest volume with the least amount of surface area (5), given the special circumstances that determine the form of each body.

Thus far, the only polyhedron which satisfied these conditions and packed with other identical units to fill space was the "tetrakaidecahedron" (Fig. 1a) of Lord Kelvin (6). This is closely re-

lated to the truncated octahedron, one of the 13 Archimedean semiregular polyhedra; it has eight doubly curved hexagonal faces and six quadrilateral faces with bowed edges. The curved surfaces are a requirement of the minimization of surface energy (7).

Matzke and Nestler (8), however, have demonstrated that the statistical distribution of polygon faces on packed soap bubbles differs markedly from Kelvin's tetrakaidecahedron in that the bubbles showed a predominance of pentagonal faces. Studies of metal crystallites (7) and vegetable cells (1) showed similar distributions (Table 1 and Fig. 2).

To date, there has apparently been no report of a polyhedron with the appropriate distribution of kinds of faces and with the ability to pack to fill space. However, such a polyhedron, the β -tetrakaidecahedron, is now proposed (Fig. 1c). It can be mechanically derived from the Kelvin polyhedron (α -tetrakaidecahedron) by taking any edge common to two hexagons plus the edges that meet at each end of this edge (Fig. 1a), rotating them 90° and reconnecting them. The resultant polyhedron (Fig. 1b) with four quadrilateral, four pentagonal, and six hexagonal faces will also pack to fill space. The same operation is then performed with the same group of edges on the opposite side of the polyhedron (Fig. 1c). This transformation retains the same number of faces (14), vertices (24), and edges (36) as the α -tetrakaidecahedron, and the vertex juncture angles remain at $109^\circ 28'$. The β -tetrakaidecahedron has two quadrilateral, eight pentagonal, and four hexagonal faces, which give an average of 5.143 sides per face.

The percentage distribution of the kinds of faces on the α -tetrakaidecahedron and the β -tetrakaidecahedron and their relationship to the distribution of faces in natural packings are shown in Table 1 and Fig. 2.

A packing of a group of β -tetrakaidecahedra is shown in Fig. 3. The packing arrangement belongs to the space group $P4_2/mnm-D_{2h}^{14}$ (9). The centers of the polyhedra correspond to special position $2a$, and the nodal points of the interstitial network correspond to positions $4d$ and $8j$ of that space group (9).

The centers of β -tetrakaidecahedra cells form a body-centered tetragonal lattice which, if the c/a axial ratio is set at unity, is equivalent to the body-centered cubic lattice. Therefore, it is

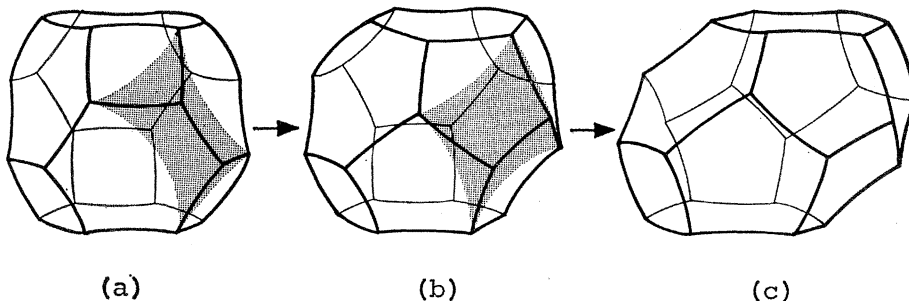


Fig. 1. The transition from the α -tetrakaidecahedron (a) through a polyhedron with four quadrilateral, four pentagonal, and six hexagonal faces (b) to the β -tetrakaidecahedron (c).